Appendix 1 Morphology of the zircons

Back-scattered electron (BSE) and cathodoluminescence (CL) images of the selected zircons analyzed by a Sensitive High mass-Resolution Ion MicroProbe (SHRIMP) II at the Beijing SHRIMP Center are shown in Fig. DR1 and U-Th-Pb data in Tables DR2, DR7 and DR8. Circles indicate location of analytical spots, whereby spot number and age with 1σ error are shown. Monzodioritic porphyry J-25 from the Jiagou intrusion is dominated by tabular euhedral zircons with inherited cores of 1700-1800, 2000 and 2400-2500Ma, and fine-scale oscillatory zoning rims with a weighted mean $^{206}Pb/^{238}U$ age 132.2±4.1Ma (2σ, MSWD=1.2, 5 analyses) (Table DR2), which agree with a magmatic origin (Hanchar and Hoskin, 2003). Fig. DR1a shows a typical zircon from this sample.

Diorite LG-1 from the Liguo intrusion is dominated by rounded and narrow banded zircons (Fig. DR1b). The former is mostly 2400-2500 Ma in age and inherited and the latter yields a weighted mean $^{206}Pb/^{238}U$ age of 131.1±3.4Ma (2σ, MSWD=1.4, 8 analyses (Table DR2)), which is identical to the magmatic age of the above Jiagou intrusion.

Although only 4 zircons were available and dated for the eclogite with the U-Pb ages of 2423±5, 2519±8, 206±15 and 125±7 Ma, respectively (Table DR 7), they

show an age pattern similar to the more abundant garnet clinopyroxenites, which is characterized by three major age peaks at 2350-2550, 210-260, and 125-136Ma (Figs. 2, DR1c and d, and DR4). The late Archean-early Proterozoic ages overlap with those of the felsic gneiss xenoliths ($^{207}Pb/^{206}Pb$ ages of 2300-2600Ma, W.L. Xu et al., 2004; Table DR8) and with the age of the NCC basements (Fig. 2). Although both the garnet clinopyroxenite xenoliths and the NCC basements show ages of 1600-2000Ma, they are not observed in the eclogite xenolith, which we attribute to the undersampling of the only 4 zircons from this sample. The early Cretaceous ages (125-136Ma) of the eclogite and garnet clinopyroxenite xenoliths are from the rim cored by Archean zircons (Fig. DR1c) and overlap with the age of the high-Mg adakitic porphyries. They show oscillatory zoning and Th/U ratios of 0.25-0.73 (Table DR7), characteristic of magmatic zircon. They clearly represent magmatic overgrowth formed during entrainment by the high-Mg adakitic magma.

The Triassic ages are characterized by very low U-Th concentrations (1-23 ppm) and therefore subjected to large analytical uncertainties in $^{206}Pb/^{238}U$ age, and the ^{207}Pb concentrations are even below detection limits (Table DR7). Seven zircons were separated and dated from garnet clinopyroxenite JG1-36 from the Jiagou intrusion. Except for the two grains with 5-6 ppm U and having very large age errors (52-170Ma, 1σ), the other 5 grains with 9-10 ppm U show consistent Triassic ages with a weighted mean $^{206}Pb/^{238}U$ age of 222±37Ma (1σ; MSWD=0.27). This age agrees with

the age of one Triassic zircon from the eclogite ($^{206}Pb/^{238}U$=206±15Ma (1σ), Table DR7). All these Triassic zircons are structureless and have Th/U ratios of typically 0.01-0.24 (Fig. DR1d; Table DR7), indicating a metamorphic origin (Hanchar and Hoskin, 2003). Although less precise, these zircon ages well agree with the garnet and whole-rock Sm-Nd isochron age of 219±5 (2σ) for the eclogite (Table DR6; Fig. DR3). They in turn agree with the age of eclogite-facies metamorphism of the Dabie-Sulu belt (220-240Ma, see text for discussion).

Felsic gneiss xenoliths from the Jiagou intrusion are dominated by rounded zircons showing patch structure or lack internal structure (Fig. DR 1e and f). The leucogneiss DJG and melagneiss EJG yield weighted mean $^{207}Pb/^{206}Pb$ ages of 2461±22Ma and 2508±15Ma, respectively, which are similar to those of inherited zircons from the host rocks, as described above (Table DR2).

Appendix 2 Estimates of pressures and temperatures

Various approaches have been used to constrain the pressure and temperature for the formation of eclogite and garnet clinopyroxenite xenoliths. The 20-29 mol% jadeite component in omphacite implies that the eclogite formed at pressures >1.5GPa (Table DR5). The observed spinel to garnet transition in garnet clinopyroxenite xenoliths (Figure DR2b) and ubiquitous presence of rutile in both

eclogite and garnet clinopyroxenite xenoliths also suggest a minimum pressure of >1.5GPa (Klemme, 2004; Xiong et al., 2005). Additionally, the observed quartz-rod exsolutions in omphacite, rutile exsolution in garnet, and aluminum-rich titanite exsolution in clinopyroxene as well as the local presence of corundum (Figure DR2c) in garnet clinopyroxenite xenoliths imply that their protoliths had been subjected to high- to ultrahigh-pressure metamorphism (~2.0-3.1GPa). It is concluded that both the eclogite and garnet clinopyroxenite xenoliths formed during eclogite-facies metamorphism. Temperatures were estimated based on the garnet-clinopyroxene Fe-Mg geothermometer (Ellis and Green, 1979; Krogh, 1988, 2000; Table DR5). Garnet and clinopyroxene compositions vary widely depending upon their occurrences. Those from samples B1-10 and L-4 (Table DR5) show negligible textural evidence of retrogression and yield temperatures ranging from 800 to 1060°C. In contrast, garnet and clinopyroxenite from retrograded samples give temperatures varying from 760 to 650°C. Omphacite and enclosing garnet from one eclogite sample (603-2-2, Table DR5) yield temperatures of 890 °C, whereas retrograded garnet and omphacite from the same sample give temperatures of 655-746 °C. We interpret the estimated high temperatures of >800 °C represent peak temperatures of eclogite-facies metamorphism leading to partial melting (see text), while the low temperatures of <750°C correspond to retrogression to amphibolite facies metamorphism during ascent and associated cooling of the host magma.

Figure DR captions

Figure DR1 Back-scattered electron (BSE) and cathodoluminescence (CL) images of zircons from Xu-Huai high-Mg adakitic intrusions J-25(a) and LG-1(b), and garnet clinopyroxenite xenoliths 603-2-1(c) and JG1-36(d), and felsic gneiss xenoliths DJG (e) and EJG (f). Except for (a) which is a BSE image, all the others are CL images.

Figure DR2 Field occurrences (a), spinel (Sp) to garnet (Grt) transition (b) and clinopyroxene (Cpx) + garnet + corundum (Co) assemblage (c) of garnet clinopyroxenite JG1-43, and garnet and amphibole (Amp) exsolutions of clinopyroxene (d) in garnet clinopyroxenite JG1-25.

Figure DR3 Garnet and whole-rock Sm-Nd isochron of eclogite 603-2-2 (see Table DR6 for data).

Figure DR4 Concordia plots for zircons from one eclogite and seven garnet clinopyroxenite xenoliths. All data were determined by SHRIMP II at the Beijing SHRIMP Center. Inset shows concordia plot for younger oscillatory magmatic overgrowth (Fig. DR1c; Table DR7). Error ellipses are shown at 1σ. The Triassic zircons from both eclogite and garnet clinopyroxenite xenoliths and the Cretaceous zircon from the eclogite xenolith are not shown because their ^{207}Pb concentrations are below detection limit.

Figure DR5 Comparison of average chondrite-normalized rare earth element compositions of the Xu-Huai eclogite (including garnet clinopyroxenite) xenoliths, their host high-Mg adakitic intrusions (ADI) and Archean metabasalts from the NCC (Gao et al., 1998). Because REE compositions in the metabaslts were determined by instrumental neutron activation analysis (Gao et al., 1998), their data on Pr, Dy, Ho, Er, and Tm are not available.

Figure DR6 Comparison of average primitive mantle normalized elemental

compositions of the Xu-Huai eclogite (including garnet clinopyroxenite) xenoliths, their host high-Mg adakitic intrusions (ADI) and Archean metabasalts from the NCC (Gao et al., 1998). The thick grey line represents melt compositions calculated by 40% batch melting of the average metabasalt in eclogite-facies with production of a residue consisting of 63% clinopyroxene, 20% garnet, 15% amphibole, 2% rutile and 0.002% zircon. It can be seen that most of the elemental compositions of the high-Mg adakitic intrusions can be interpreted by this melt composition. Partition coefficients were taken from Pertermann et al. (2004) for clinopyroxene and garnet, from Bacon and Druitt (1988), Ewart and Griffin (1994) and Sisson (1994) for amphibole, and from Jenner et al. (1994) and Foley et al. (2000) for rutile. A Zr partition coefficient of ~1600 between zircon and melt is assumed based on Zr concentrations in zircon (49.76 wt%) and melt (<300 ppm). A similar partition coefficient for Hf is assumed.

Figure DR7 Sr–Nd isotopic compositions of the Early Cretaceous Xu-Huai high-Mg adakitic intrusions compared to the Xu-Huai (XH) eclogite and garnet clinopyroxenite xenoliths (filled triangles; large open triangle with error bars indicates the median value with 1σ error) and the late Jurassic Xinglonggou high-Mg adakites, dacites and andesites (Gao et al., 2004). The thick black curves with pluses are AFC (assimilation and fractional crystallization) trends showing 10% increments in F (magma remaining) for a 40% partial melt of the median Xu-Huai eclogite-garnet clinopyroxenite that assimilates mantle (DM; Salters and Stracke, 2004). The two trends represent melts derived from the xenoliths with the highest (upper curve) and lowest (lower curve) Sr-Nd contents, respectively. The eclogitic residue is assumed to consist of 63% clinopyroxene, 20% garnet, 15% amphibole, 2% rutile and 0.002% zircon, as in

Figure DR6. The AFC model assumes a ratio of the rate of assimilation to the rate of fractional crystallization (r) close to 1.0 and the reacted mantle to be comprised of 40% garnet, 40% orthopyroxene and 20% clinopyroxene without olivine, in agreement with experimental and empirical studies (Rapp et al., 1999; Prouteau et al., 2001). However, the presence of olivine has little effect on the results, due to its low Sr and Nd partition coefficients in intermediate melts (similar to those of orthopyroxene) (Fujimaki et al., 1984; Dunn & Sen, 1994; Bacon & Druitt, 1988). The trend is not very sensitive to the initial melt composition determined by the degree of partial melting of the median Xu-Huai eclogite-garnet clinopyroxenite, nor to the relative mineral proportions of the residues and the reacted mantle. As shown in Gao et al. (2004), initial melt compositions from 10-50% partial melting and a garnet proportion from 10 to 80% also yield trends through the Xinglonggou data, with F ranging from 75 to 90%. The Sr-Nd isotopic compositions of the Xinglonggou lavas are consistent with consumption of <40% melt during reaction with the mantle and with negligible crustal assimilation (Gao et al., 2004).

Grey lines show energy-constrained assimilation and fractional crystallization (EC-AFC; Bohrson and Spera, 2001) trends for assimilation of the median Xinglonggou lava (solid grey lines) and the Xinglonggou lava with least radiogenic Sr (dash grey lines) by the North China crust (NCC; Wu et al., 2005). The crystallizing mineral assemblage is assumed to consist of 35% plagioclase, 30% quartz, 20%

amphibole, 10% K-feldspar, and 5% biotite based on mineral assemblages of the Xu-Huai intrusions. Since the modeling results depend to a large extent upon Sr-Nd partition coefficients between crystallizing plagioclase and melt, two suites of partition coefficients obtained by Bea et al. (1994) and Dun and Sen (1994) are used and their results correspond to the upper curve and lower curve, respectively, in both cases. The EC-AFC models assume equilibration temperatures (Teq) (i.e., the final temperature to which the magma cools and the wallrock heats up) of 800°C. Sr-Nd partition coefficients for K-feldspar and biotite were from Bea et al. (1994) and those for amphibole from Sisson (1994). It can be seen that the Xu-Huai adakitic intrusions have Sr-Nd isotopic compositions which either agree with those of the Xu-Huai eclogite and garnet clinopyroxenite xenoliths within errors or with those of the Xinglonggou lavas followed by an EC-AFC process in the NCC.

Reference not cited in main paper

Bacon, C.R., and Druitt, T.H., 1988, Compositional evolution of the zoned calcalkaline magma chamber of Mount-Mazama, Crater Lake, Oregon: Contributions to Mineralogy and Petrology, v.98, 224-256.

Bea, F., Pereira, M. D., and Stroh, A., 1994, Mineral/leucosome trace-element partitioning in a peraluminous migmatite (a laser ablation-ICP-MS study): Chemical Geology, v. 117, p. 291-312.

Bohrson, W.A., and Spera, F.J., 2001, Energy-constrained open-system magmatic processes II: Application of energy-constrained assimilation-fractional crystallization (EC-AFC) model to magmatic systems: Journal of Petrology, v. 42, p. 1019–1041.

Dun, T., and Sen, C., 1994, Mineral/matrix partition coefficients for orthopyroxene, plagioclase, and olivine in basaltic to andesitic systems: a combined analytical and experimental study. Geochimica et Cosmochimica Acta, v. 58, p. 717–733.

Ellis, D.J., and Green, D.H., 1979, An experimental study of the effect of Ca upon garnet-clinopyroxene Fe-Mg exchange equilibria: Contributions to Mineralogy and Petrology, v. 71, p. 13-22.

Ewart, A., and Griffin, W.L., 1994, Application of proton-microprobe data to trace-element partitioning in volcanic-rocks: Chemical Geology, v.117, p. 251-284.

Foley, S.F., Barth, M.G., and Jenner, G.A., 2000, Rutile/melt partition coefficients for trace elements and an assessment of the influence of rutile on the trace element characteristics of subduction zone magmas: Geochimica et Cosmochimica Acta, v. 64, p. 933-938.

Fujimaki, H., Tatsumoto, M., and, Aoki, K., 1984, Partition coefficients of Hf, Zr, and REE between phenocrysts and groundmass: Proc.14th Lunar Planet. Sci. Conf. Part 2, Journal of Geophysical Research, v. 89 (suppl), p. 662-672.

Hanchar, J,M. & Hoskin, P.W.O. (eds), 2003. Zircon: Reviews in Mineralogy & Geochemistry, v. 53, Mineralogical Society of America and Geochemical Society, pp.500.

Jenner, G.A., Foley, S.F., Jackson, S.E., Green, T.H., Fryer, B.J., and Longerich, H.P., 1994, Determination of partition coefficients for trace elements in high

pressure-temperature experimental run products by laser ablation microprobe-inductively coupled plasma-mass spectrometry (LAM-ICP-MS): Geochimica et Cosmochimica Acta, v.58, p.5099-5103.

Klemme, S., 2004, The influence of Cr on the garnet–spinel transition in the Earth's mantle: experiments in the system $MgO–Cr_2O_3–SiO_2$ and thermodynamic modeling: Lithos, v. 77, p. 639–646, doi: 10.1016/j.lithos.2004.03.017.

Krogh, E. J., 1988, The garnet-clinopyroxene Fe-Mg geothermometer-a reinterpretation of existing experimental data: Contributions to Mineralogy and Petrology, v. 99, p. 44-48.

Krogh, R. E., 2000, Distribution of Fe^{2+} and Mg between coexisting garnet and hornblende in synthetic and natural systems: an empirical calibration of the garnet-hornblende Fe-Mg geothermometer: Lithos, v. 53, p. 265-277.

Pertermann, M., Hirschmann, M. M., Hametner, K., Günther, D., and Schmidt, M.W., 2004, Experimental determination of trace element partitioning between garnet and silica-rich liquid during anhydrous partial melting of MORB-like eclogite: Geochemistry, Geophysics and Geosystems, v.5, Q05A01, doi: 10. 1029/2003 GC000638.

Prouteau, G., Pichavant, M., and Maury, R.C., 2001, Evidence for mantle metasomatism by hydrous silicic melts derived from subducted oceanic crust: Nature, v. 410, p. 197-200.

Rapp, R.P., Shimizu, N., Norman, M. D., and Applegate, G.S., 1999, Reaction between slab-derived melts and peridotite in the mantle wedge: experimental constraints at 3.8 GPa: Chemical Geology, v. 160, p. 335-356.

Salters, V.J.M. and Stracke, A., 2004, Composition of the depleted mantle: Geochemistry, Geophysics and Geosystems, v. 5, Q05004, doi: 10.1029/2003GC000597.

Sisson, T.W., 1994, Hornblende-melt trace-element partitioning measured by ion microprobe: Chemical Geology, v. 117, p. 331-344.

Wu, F. Y., Zhao, G. C.., Wilde, S. A. and Sun, D. Y., 2005, Nd Isotopic constraints on the crustal formation of the North China Craton: Journal of Asian Earth Sciences, v.24, p.523-545.

Table DR 1. Major (wt.%) and trace element (ppm) and Sr-Nd isotopic data of Early Cretaceous porphyries from the Xu-Huai area

Intrusion	Liguo			Banjing						Jiagou			
Sample No.	L-7	LG1-1	LG3-8	064-1	8102-389	8201-69-10	8201-69-2	8202-392	74	J-25	JG4-3	JG4-4	JG4-18
Latitude	34°33'03"	34°34'26"	34°33'07"	34°08'58"	34°09'48"	34°09'50"	34°09'45"	34°09'40"	34°08'55"	33°52'42"	33°52'43"	33°52'42"	33°52'42"
Longitude	117°19'03"	117°18'55"	117°18'00"	117°05'40"	117°04'25"	117°04'22"	117°04'30"	117°04'42"	117°05'38"	117°00'54"	117°00'55"	117°00'56"	117°00'54"
Rock type	D		Q-M	M-D	Q-M	Hb-D	M-D	D		M-D	D	D	D
SiO_2	60.88	60.74	67.18	59.08	66.57	55.33	61.73	60.7	60.58	61.41	60.88	60.22	60.95
TiO_2	0.61	0.62	0.3	0.62	0.34	0.83	0.47	0.61	0.6	0.58	0.55	0.59	0.53
Al_2O_3	14.34	13.69	14.63	17.57	15.23	16.8	17.14	14.85	14.84	15.06	15.62	15.78	15.53
Fe_2O_3	3.14	2.83	1.11	3.25	1.55	3.88	1.93	2.87	2.52	2.29	5.96	6.24	6.02
FeO	3.34	3.92	1.75	2.37	2.15	4.33	1.93	3.8	3.53	4.03			
MnO	0.11	0.12	0.07	0.08	0.09	0.14	0.06	0.14	0.09	0.11	0.08	0.08	0.08
MgO	4.68	5.73	1.47	2.88	2.34	4.71	3.05	4.59	4.59	3.44	3.51	4.23	3.54
CaO	5.58	5.43	3.1	4.88	3.25	7.33	4.69	5.68	4.43	5.54	5.32	5.30	5.32
Na_2O	5.12	3.71	4.69	5.1	5.16	3.95	5.43	4.05	4.42	4.28	4.33	3.90	4.22
K_2O	0.89	2.12	2.62	2.37	2.57	1.14	2.21	1.73	2.17	2.28	2.33	2.33	2.32
P_2O_5	0.16	0.18	0.09	0.24	0.12	0.25	0.15	0.17	0.16	0.17	0.16	0.18	0.16
LOI	0.93	0.68	2.75	2.06	0.35	1.25	1.03	0.55	2.38	0.49	0.76	0.96	0.85
Total	99.78	99.77	99.76	100.5	99.72	99.94	99.82	99.74	100.3	99.68	99.50	99.81	99.52
$Mg^{\#}$ [a]	58	61	49	49	54	52	60	56	59	50	54.00	57.00	54.00
La	14.25	18.25	11.45	26.25	16.59	16.9	21.58	18.39	14.68	25.85	24.32	22.50	23.78
Ce	32.32	38.33	25.33	56.77	32.81	41.31	42.67	37.77	32.37	58.98	46.92	43.86	45.23
Pr	4.21	5	3.46	6.78	4.21	5.39	4.78	4.87	3.94	5.41	5.22	4.97	5.01
Nd	17.41	19.31	13.92	26.03	16.3	22.26	17.26	18.36	16.19	20.33	21.26	20.57	20.41
Sm	3.66	3.7	2.88	4.57	3.19	4.35	2.95	3.4	3.18	4.11	4.05	4.03	3.86
Eu	1.11	0.94	0.73	1.27	0.82	1.17	0.94	0.94	0.9	1.25	1.27	1.25	1.22
Gd	3.46	2.92	2.01	3.28	2.14	3.65	2.26	2.86	2.69	3.51	3.76	3.65	3.58
Tb	0.5	0.43	0.24	0.46	0.28	0.52	0.31	0.44	0.37	0.49	0.50	0.50	0.48
Dy	2.84	2.3	1.05	2.54	1.33	3.11	1.72	2.39	2.21	2.73	2.68	2.70	2.59
Ho	0.54	0.44	0.17	0.48	0.24	0.6	0.33	0.47	0.43	0.53	0.55	0.55	0.53
Er	1.58	1.16	0.48	1.39	0.67	1.78	0.9	1.3	1.15	1.58	1.46	1.45	1.42
Tm	0.22	0.17	0.08	0.22	0.1	0.27	0.14	0.2	0.18	0.22	0.22	0.22	0.22
Yb	1.45	1.11	0.48	1.29	0.7	1.65	0.89	1.3	1.13	1.52	1.53	1.51	1.48
Lu	0.19	0.17	0.08	0.21	0.14	0.27	0.15	0.21	0.18	0.21	0.24	0.23	0.23
Y	14.41	11.83	4.84	13.83	7.01	17.6	9.23	13.16	12.67	14.64	16.78	16.95	16.82
Rb	13.17	65.43	64.63	51.8	52.5	28	39.9	49.4	49.2	62.21	55.66	56.76	54.17
Sr	617.8	510	452	841	861	629	1052	616	535	1180	1,066	954	1,079

Table DR 1(continued)

Intrusion	Liguo			Banjing						Jiagou			
Sample No.	L-7	LG1-1	LG3-8	064-1	8102-389	8201-69-10	8201-69-2	8202-392	74	J-25	JG4-3	JG4-4	JG4-18
Latitude	34°33'03"	34°34'26"	34°33'07"	34°08'58"	34°09'48"	34°09'50"	34°09'45"	34°09'40"	34°08'55"	33°52'42"	33°52'43"	33°52'42"	33°52'42"
Longitude	117°19'03"	117°18'55"	117°18'00"	117°05'40"	117°04'25"	117°04'22"	117°04'30"	117°04'42"	117°05'38"	117°00'54"	117°00'55"	117°00'56"	117°00'54"
Rock type	D		Q-M	M-D	Q-M	Hb-D	M-D	D		M-D	D	D	D
Ba	408.9	592	827	704	886	575	1264	664	567	1578	1,301	1,251	1,286
Nb	3	4.48	2.36	7.3	3.23	6.7	5.2	4.27	5.9	6.12	6.65	6.79	6.11
Ta	-	0.33	0.14	-	0.22	-	-	0.28	-	0.11	0.46	0.51	0.43
Zr	69.88	53.61	99.81	142	113	106	117	127.8	106	192.9	118.08	116.69	114.77
Hf	2.19	1.49	3.18	-	3.08	-	-	3.14	-	5.55	3.36	3.37	3.31
Th	2.78	4.86	3.44	2	3.88	10.2	2	3.51	-	8.07	8.44	7.27	8.19
U	1.14	1.27	1.31	-	1.42	-	-	0.93	7.9	3.61	3.63	2.86	3.86
Sc	18.32	15.75	4.71	-	6.06	-	-	14.9	-	17	17.08	17.58	18.00
V	208.9	116.6	55.15	-	69.4	-	-	132.2	-	133.2	124.28	128.94	125.69
Cr	214.3	228.3	66.65	-	116.5	59	96	187	157	106.3	122.00	158.00	125.00
Co	25.86	25.32	7.93	35	11.28	-	-	23.84	-	19.01	73.78	98.76	76.56
Ni	103.73	133.5	25.18	16.3	44.82	22.9	42.2	80.72	82.9	35.37	43.24	65.87	43.92
$(La/Sm)_N$	2.52	3.19	2.57	3.72	3.36	2.52	4.74	3.5	2.99	4.07	3.78	3.51	3.88
$(La/Yb)_N$	6.84	11.42	16.6	14.13	16.55	7.11	16.84	9.85	9.02	11.78	10.72	10.05	10.83
Sr/Y	42.9	43.1	93.6	60.8	122.9	35.7	114	46.8	42.2	80.6	63.5	56.3	64.2
$^{87}Rb/^{86}Sr$	0.199	0.39	0.407		0.184		0.097	0.215		0.141			
$^{87}Sr/^{86}Sr$	0.707519	0.70625	0.70695		0.705685		0.706	0.706416		0.707738	0.707712	0.708087	0.708363
$2\sigma(\times10^{-6})$	22	20	14		15		19	18		14	6	20	16
$^{147}Sm/^{144}Nd$	0.1248	0.1207	0.1339		0.1252		0.1093	0.1195		0.1168			
$^{143}Nd/^{144}Nd$	0.512117	0.512248	0.512346		0.512349		0.511889	0.512047		0.51203	0.512008	0.512028	0.512003
$2\sigma(\times10^{-6})$	8	11	10		8		10	9		8	4	4	5
I_{Sr} (130Ma)	0.7071	0.7055	0.7062		0.7053		0.7058	0.706		0.7075			
$\varepsilon_{Nd}(130Ma)^b$	-8.95	-6.33	-4.64		-4.43		-13.14	-10.23		-10.52			
T_{DM} (Ma)^b	1766	1476	1533		1378		1836	1780		1757			
$f_{Sm/Nd}$	-0.37	-0.39	-0.32		-0.36		-0.44	-0.39		-0.41			

a. $Mg^{\#}$ = molar 100 ($Mg/Mg+Fe^{2+}$), where FeO = FeO+0.9 Fe_2O_3. b. The present-day $^{143}Nd/^{144}Nd$ and $^{147}Sm/^{144}Nd$ values used are 0.512638 and 0.1967 for chondrite and 0.51315 and 0.222 for depleted mantle.
-: Not determined and /or below detecting limit. D: dioritic porphyry; Hb-D: hornblende-dioritic porphyry; M-D: Monzodioritic porphyry; Q-M: Quartz monzonitic porphyry.

Table DR 2 SHRIMP zircon U-Pb data on monzodioritic porphyry and diorite

Rock	Spot	U ppm	Th ppm	Th /U ratio	$^{206}Pb^*$ ppm	f206 %	$^{207}Pb^*/^{235}U$	1 σ
Jiagou monzodioritic porphyry J25	J25-1.1	508	420	0.85	144	0.05	4.97	0.1342
	J25-2.1	137	74	0.56	44.9	0.17	6.8	0.1768
	J25-3.1	114	5	0.05	2.5	3.73	0.131	0.0328
	J25-4.1	31	7	0.22	14.6	0.69	14.21	0.6110
	J25-4.2	411	37	0.09	188	0.04	12.5	0.3000
	J25-3.2	56	4	0.07	1.32	10.13		0.0000
	J25-5.1	665	105	0.16	211	0.08	5.82	0.1630
	J25-1.2	1348	169	0.13	25	0.7	0.1365	0.0053
	J25-6.1	410	117	0.3	142	0.2	6.71	0.1678
	J25-7.1	627	205	0.34	273	0.05	11.67	0.4085
	J25-7.2	1194	260	0.23	21.3	0.95	0.1227	0.0054
	J25-8.1	211	113	0.55	65.2	0.18	6.45	0.1871
	J25-9.1	185	90	0.5	55.1	0.14	5.91	0.1418
	J25-9.2	495	198	0.41	120	0.22	4.156	0.0997
	J25-10.1	830	187	0.23	179	0.11	3.64	0.0837
	J25-10.2	1084	109	0.1	19.8	1.18	0.167	0.0073
	J25-11.1	178	141	0.82	36.9	0.04	3.502	0.0876
	J25-11.2	142	14	0.1	3.04	2.18	0.163	0.0261
	J25-12.1	94	40	0.44	23.2	0.14	4.4	0.1144
	J25-12.2	1061	393	0.38	19	0.06	0.1447	0.0043
	J25-13.1	225	165	0.76	89.3	0.06	11.17	0.2681
	J25-13.2	502	176	0.36	190	0.03	10.45	0.2404
	J25-14.1	2385	145	0.06	644	0.01	4.88	0.1074
	J25-14.2	3271	198	0.06	56.3	0.11	0.1384	0.0035
Liguo diorite LG1	LG1-1.1	119	58	0.5	23.2	0.37	4.8	0.1200
	LG1-2.1	134	95	0.73	2.42	2.07	0.132	0.0172
	LG1-3.1	492	451	0.95	8.96	0.57	0.1397	0.0073
	LG1-4.1	190	166	0.9	3.25	2	0.128	0.0141
	LG1-5.1	93	79	0.87	1.66	1.72	0.172	0.0258
	LG1-6.1	120	64	0.55	47.2	0.14	10.63	0.2551
	LG1-7.1	412	502	1.26	7.25	0.13	0.1487	0.0062
	LG1-8.1	381	347	0.94	6.99	1.49	0.155	0.0116
	LG1-9.1	75	52	0.72	1.34	3.14	0.132	0.0185
	LG1-10.1	50	34	0.7	1.04	8.14	0.283	0.0679
	LG1-11.1	362	126	0.36	150	0.03	10.76	0.2475
	LG1-11.2	288	103	0.37	122	0.05	11.35	0.2611
	LG1-12.1	360	92	0.26	140	0.02	11.1	0.2553
	LG1-13.1	31	28	0.93	13.9	0.67	11.25	0.3600
	LG1-14.1	34	30	0.91	13.9	0.21	10.75	0.2903
	LG1-15.1	315	65	0.21	117	0.02	8.9	0.2047

* Radiogenic Pb.

f206% is (common ^{206}Pb/total ^{206}Pb) x 100.

Table DR 2 (continued)

Rock	Spot	Atomic ratio				Ages (Ma)			
		$^{206}Pb^{*}/^{238}U$	1 σ	$^{207}Pb^{*}/^{206}Pb^{*}$	1 σ	$^{206}Pb/^{238}U$	1 σ	$^{207}Pb/^{206}Pb$	1 σ
Jiagou	J25-1.1	0.3295	0.0089	0.10947	0.0005	1,836	±43	1791	± 8.1
monzodioritic	J25-2.1	0.3811	0.0088	0.1294	0.0016	2,082	±41	2090	± 21
porphyry	J25-3.1	0.02449	0.0007	0.0388	0.0097	155.9	± 4.3	-432	±660
J25	J25-4.1	0.538	0.0140	0.1915	0.0065	2,776	±59	2755	± 56
	J25-4.2	0.533	0.0123	0.1701	0.0015	2,753	±51	2559	± 14
	J25-3.2	0.02453	0.0010		0.0000	156.2	± 6.3		
	J25-5.1	0.3693	0.0085	0.1142	0.0019	2,026	±39	1868	± 31
	J25-1.2	0.0214	0.0005	0.0463	0.0015	136.5	± 3.1	12	± 77
	J25-6.1	0.4008	0.0096	0.12141	0.0008	2,173	±44	1977	± 13
	J25-7.1	0.507	0.0137	0.1671	0.0037	2,642	±58	2529	± 37
	J25-7.2	0.02057	0.0005	0.0433	0.0016	131.2	± 3.1	-152	± 93
	J25-8.1	0.3593	0.0097	0.1301	0.0013	1,979	±47	2099	± 18
	J25-9.1	0.3471	0.0080	0.12356	0.0009	1,921	±38	2008	± 13
	J25-9.2	0.2812	0.0065	0.10717	0.0007	1,598	±32	1752	± 13
	J25-10.1	0.2509	0.0055	0.10522	0.0004	1,443	±29	1718	± 7.3
	J25-10.2	0.02097	0.0005	0.0578	0.0021	133.8	± 3.0	521	± 82
	J25-11.1	0.2408	0.0055	0.10547	0.0009	1,391	±29	1722	± 17
	J25-11.2	0.02442	0.0007	0.0484	0.0077	155.5	± 4.3	117	±370
	J25-12.1	0.2874	0.0066	0.111	0.0011	1,629	±34	1815	± 19
	J25-12.2	0.02079	0.0005	0.05048	0.0010	132.7	± 3.0	217	± 45
	J25-13.1	0.462	0.0106	0.17534	0.0008	2,449	±47	2609	± 7.4
	J25-13.2	0.4395	0.0097	0.1724	0.0005	2,348	±44	2581	± 5.2
	J25-14.1	0.3143	0.0069	0.11267	0.0002	1,762	±34	1843	± 3.5
	J25-14.2	0.02	0.0004	0.05017	0.0006	127.6	± 2.8	203	± 27
Liguo	LG1-1.1	0.2263	0.0052	0.1538	0.0013	1,315	±28	2388	± 14
diorite	LG1-2.1	0.02056	0.0005	0.0464	0.0060	131.2	± 3.4	19	±320
LG1	LG1-3.1	0.02107	0.0005	0.0481	0.0022	134.4	± 3.2	103	±110
	LG1-4.1	0.01952	0.0005	0.0477	0.0052	124.6	± 3.2	85	±250
	LG1-5.1	0.02029	0.0006	0.0614	0.0086	129.5	± 3.7	654	±310
	LG1-6.1	0.457	0.0105	0.1687	0.0011	2,426	±47	2545	± 11
	LG1-7.1	0.02049	0.0005	0.0526	0.0018	130.8	± 3.0	313	± 80
	LG1-8.1	0.02106	0.0005	0.0534	0.0038	134.4	± 3.2	346	±160
	LG1-9.1	0.02026	0.0006	0.0472	0.0061	129.3	± 3.7	60	±320
	LG1-10.1	0.02205	0.0009	0.093	0.0223	140.6	± 5.6	1488	±450
	LG1-11.1	0.484	0.0111	0.16114	0.0007	2,545	±48	2468	± 7.7
	LG1-11.2	0.493	0.0113	0.16685	0.0007	2,586	±48	2526	± 6.5
	LG1-12.1	0.452	0.0104	0.1782	0.0007	2,402	±46	2636	± 6.3
	LG1-13.1	0.51	0.0133	0.1601	0.0030	2,655	±56	2457	± 31
	LG1-14.1	0.471	0.0118	0.1655	0.0020	2,488	±51	2513	± 20
	LG1-15.1	0.432	0.0099	0.14944	0.0006	2,315	±44	2340	± 6.6

Table DR 3 Texture and modal mineral compositions (%) based on point-counting of the eclogite and garnet clinopyroxenite xenoliths

			Mineral content (%)							
Sample No.	Lithology	Texture	Grt	Cpx	Amp	Pl	Ru	Sph	Q	Opaque
603-2-2	Eclogite	Granoblastic	35	52	10 (Re)		3			
B1-10	Eclogite	Granoblastic	40	45	8 (Pr)		2		5	
L-4	Eclogite	Granoblastic	30	68						2
603-2-1	Grt-pyr.	Granoblastic	56	30	10 (Re)		1			3
JG1-36	Grt-pyr.	Granoblastic	28	32	4 (Re)	20	2	4 (Re)	10	
JG3-52	Grt-pyr.	Granoblastic	35	45	10 (Re)	5	1	2	2	
JG3-65	Grt-Pl-pyr.	Granoblastic	20	35	8 (Re)	27	2	4 (Re)	4	
JG3-31	Grt-pyr.	Granoblastic	38	50	6 (Re)	5	1			
JG2-38	Grt-pyr.	Granoblastic	45	45	7 (Re)	2	1			

Amp-amphibole, Cpx-clinopyroxene, Ex-exsolution, Grt-garnet, Pl-plagioclase, Pr-primary, Pyr-pyroxenite, Q-quartz, Re-retrograded, Ru-rutile, Sph-sphene.

Table DR 4 Mineral chemical compositions of eclogite and garnet clinopyroxenite xenoliths

Sample No.	603-2(-2)								B1-10								
Mineral	Grt1-c	Grt1-r	Grt2-c	Grt2-r	Omph2	Omph1	Omph3	Amp*	Grt1-c	Grt1-r	Grt2-c	Grt2-r	Omph2-c	Omph2-r	Omph1	Omph3	Amp**
SiO_2	37.66	39.2	39.13	38.67	51.78	52.94	52.78	40.56	40.35	39.67	39.86	40.01	53.19	53.86	54.7	52.56	43.75
TiO_2	-	0.05	0.04	0.01	0.48	0.31	0.53	2.36	-	0.04	0.06	-	0.31	0.37	0.45	0.65	0.75
Al_2O_3	24	23	22.04	21.96	8.19	8.84	9.56	16.37	22.1	24.2	22.32	22.5	8.22	8.73	9.83	9.6	16.63
Cr_2O_3	0.3	-	0.09	0.16	0.04	0.06	0	0.04	0.14	0.2	0.15	0.11	0.03	0.09	-	0.09	0.14
FeO	20.22	20.54	20.96	20.88	6.26	5.37	5.62	13.77	16.83	16.57	17.78	18.56	4.92	3.82	4.2	3.95	5.77
MnO	0.62	0.47	0.54	0.5	0.05	-	0.14	0.07	0.17	0.43	0.35	0.42	0.03	-	0.02	0.2	0.07
MgO	8.78	8.33	8.5	8.35	10.76	11.38	11.08	11.71	11.3	11.1	12.02	10.06	11.9	11.71	11.56	11.63	16.45
CaO	8.49	8.37	8.97	8.96	18.11	17.2	16.48	10.18	9.06	7.79	7.62	8.82	18.41	18.81	15.4	17.68	10.38
Na_2O	0.04	-	0.04	0.08	3.8	3.9	3.77	2.72	-	-	0.05	-	3.43	3.51	3.85	3.63	3.28
K_2O	-	-	-	-	-	-	0.03	0.23	-	-	0.02	0.05	-	-	-	0.04	0.81
Total	100.1	99.95	100.31	99.57	99.47	100	99.99	98.01	100.02	100.02	100.03	100.53	100.44	100.96	100.01	100.03	98.03
Si	2.902	2.968	3	2.996	1.884	1.906	1.906	5.815	3.019	2.935	3.003	3	1.91	1.922	1.965	1.889	6.088
Ti	-	0.003	0.002	0.001	0.013	0.008	0.014	0.255	-	0.002	0.003	-	0.008	0.01	0.012	0.018	0.079
Al	2.177	2.052	1.99	2.003	0.352	0.375	0.406	2.764	1.947	2.108	1.98	1.987	0.348	0.367	0.416	0.407	2.726
Cr	0.018	-	0.005	0.01	0.001	0.002	-	0.005	0.008	0.012	0.009	0.007	0.001	0.003	-	0.003	0.015
Fe^{3+}	0.358	0.327	0.414	0.214	0.12	0.065	0.017	1.167	0.48	0.355	0.46	0.496	0.052	0.009	-	0.031	0.672
Fe^{2+}	1.146	1.328	1.253	1.237	0.071	0.097	0.153	0.484	1.027	1.075	1.01	1.146	0.096	0.105	0.126	0.088	-
Mn	0.04	0.03	0.035	0.033	0.002	-	0.004	0.009	0.011	0.027	0.022	0.027	0.001	-	0.001	0.006	0.008
Mg	1.009	0.94	0.971	0.964	0.584	0.611	0.596	2.503	1.26	1.224	1.35	1.125	0.637	0.623	0.607	0.623	3.413
Ca	0.701	0.679	0.737	0.744	0.706	0.664	0.638	1.564	0.726	0.617	0.615	0.709	0.708	0.719	0.593	0.681	1.548
Na	0.006	-	0.006	0.012	0.268	0.272	0.264	0.756	-	-	0.007	-	0.239	0.243	0.268	0.253	0.885
K	-	-	-	-	-	-	0.001	0.042	-	-			-	-	-	0.002	0.144
Alm	39.8	44.6	41.7	42					34	36.5	34	38.1					
Pyr	34.7	31.6	32.5	32.1					41.7	41.6	44.8	37.4					
Gross	9.9	10.1	8.3	15.6					5.4	6.9	2.8	4.8					
And	13.4	12.7	16	8.7					18.2	13.6	17.3	18.5					
Spess	1.4	1	1.2	1.1					0.4	0.9	0.7	0.9					
Uvaro	0.8	0	0.3	0.5					0.3	0.5	0.4	0.3					
WEF					71.8	71.6	72.5						75.1	74.9	71.4	73.4	
Jd					18.7	23.1	26.1						20.7	24.4	28.6	24.1	
Ae					9.5	5.3	1.4						4.2	0.7	0	2.5	

Note: Amp*-retrograde amphibole; Amp**-primary amphibole; Aug-augite; Grt-garnet; Omph-omphacite. Numbers after minerals denote analyzed grains. c-core; r-rim. Ae-aegirine; Alm-almandine; And-andradite;Gross-grossular; Jd-jadeite; Pyr-pyrope;Spess-spessartine; Uvaro-uvarovite; WEF-augite. -: below detection limit.

Table DR 4 (continued)

Sample No.	L-4				603(-2-1)		JG1-36				JG3-65		JG2-38		JG3-52			JG3-31		
Mineral	Grt-1	Grt-2	Omph1	Omph2	Grt	Aug	Grt-c	Grt-r	Aug-r	Aug-c	Grt	Aug	Grt	Aug	Grt	Aug	Amp*	Grt	Aug	Amp*
SiO_2	41.59	40.12	49.69	52.38	38.24	50.52	38.74	38.89	53.28	53.57	39.15	52.45	39.71	51.63	36.68	49.87	43	36.27	54.3	42.39
TiO_2	0.05	0.05	0.72	0.68	0.15	0.56	-	0.02	0.17	0.25	-	0.32	-	0.42	0.02	0.21	0.34	0.07	0.22	0.02
Al_2O_3	22.6	22.3	7.85	8.15	21.1	5.35	22.02	22.16	3.29	3.31	22.54	4.52	22.16	6.86	26.45	5.74	16.72	25.65	4.31	15.32
Cr_2O_3	-	0.16	-	0.08	-	0.14	0.07	0.01	-	0.03	-	0.04	0.08	-	-	-	-	-	-	0.06
FeO	16.69	19.12	6.85	6.42	25.3	9.9	24.44	23.29	5.37	5.96	22.61	6.87	24.26	6.82	22.66	6.56	13.24	25.57	8.48	17.77
MnO	0.79	0.6	-	0.12	1.01	0.13	0.57	0.3	0.06	0.12	0.53	-	0.29	0.04	0.52	0.05	-	0.51	0.12	0.14
MgO	12.8	12.1	12.16	11.24	5.97	11.19	8.15	7.22	14.14	13.83	7.75	12.89	5.39	11.18	8.76	15.04	11.57	7.51	13.21	9.18
CaO	5.58	6.48	19.63	18.21	8.27	20.64	6.35	8.45	22.34	22.35	6.61	21.85	8.1	21.04	4.91	20.95	9.76	4.39	17.48	10.25
Na_2O	-	-	3.13	2.69	-	1.65	-	0.03	1.18	1.28	0.06	1	-	1.96	-	1.49	2.5	-	1.62	1.78
K_2O	-	-	-	0.05	-	-	-	-	-	-	-	-	-	-	-	-	0.5	-	-	0.74
Total	100.1	100.93	100.03	100.02	100.04	100.1	100.3	100.4	99.83	100.7	99.25	99.94	100	99.96	100	99.92	97.64	99.96	99.75	97.67
Si	3.026	3.006	1.8	1.912	3.01	1.876	2.993	2.993	1.953	1.951	2.988	1.936	3.007	1.899	2.804	1.812	6.125	2.819	2.06	6.265
Ti	0.003	0.003	0.02	0.019	0.009	0.016	-	0.001	0.005	0.007	-	0.009	-	0.012	0.001	0.006	0.036	0.004	0.006	0.002
Al	1.937	1.967	0.335	0.351	1.956	0.234	2.004	2.009	0.142	0.142	2.026	0.197	1.976	0.297	2.382	0.246	2.805	2.347	0.187	2.667
Cr	-	0.009	-	0.002	-	0.004	0.004	0.001	-	0.001	-	0.001	0.005	-	-	-	-	-	-	0.007
Fe^{3+}	0.329	0.474	-	-	0.105	0.097	0.678	0.719	0.026	0.031	0.264	-	0.366	0.021	0.335	-	1.112	0.1	-	0.577
Fe^{2+}	1.163	1.105	0.207	0.196	1.56	0.21	1.497	1.447	0.139	0.151	1.52	0.212	1.729	0.188	1.378	0.2	0.465	1.561	0.262	1.62
Mn	0.049	0.038	0	0.004	0.067	0.004	0.037	0.02	0.002	0.004	0.034	-	0.019	0.001	0.034	0.002	-	0.034	0.004	0.018
Mg	1.388	1.351	0.657	0.612	0.701	0.619	0.939	0.828	0.773	0.751	0.882	0.709	0.608	0.613	0.998	0.815	2.457	0.87	0.727	2.023
Ca	0.435	0.52	0.762	0.712	0.697	0.821	0.526	0.697	0.877	0.872	0.541	0.864	0.657	0.829	0.402	0.816	1.49	0.366	0.692	1.623
Na	-	-	0.22	0.19	-	0.119	-	0.004	0.084	0.09	0.009	0.072	-	0.14	-	0.105	0.69	-	0.116	0.51
K	-	-	-	0.002	-	-	-	-	-	-	-	-	-	-	-	-	0.091	-	-	0.14
Alm	36.7	38.3			51.5		51.1	48.9					57.4		49			55.2		
Pyr	44.8	45.8			23.2		30.6	27.1					20.2		35.5			30.7		
Gross	0.2	2.9			18		16.4	23					6		1			8.5		
And	16.6	11.4			5.1		0.6	0.3					15.6		13.3			4.4		
Spess	1.3	1.6			2.2		1.2	0.6					0.6		1.2			1.2		
Uvaro	0.4	0			0		0.1	0.1					0.2		0			0		
WEF			78.7	80		88.1			91.4	90.8		92.6		85.4		89.7			87.9	
Jd			21.3	20		11.9			6.7	6.9		7.4		13.2		10.3			12.1	
Ae			0	0		0			1.9	2.3		0		1.4		0			0	

Table DR 5 Estimated P-T conditions for the xenoliths

Sample	Used mineral pair	Eclogite-facies metamorphism		
		T (ºC)		
		Ellis and Green (1979) Grt-Cpx (P=15kb)	Krogh (2000) Grt-Cpx (P=15kb)	Krogh (1988) Grt-Cpx (P=15kb)
		Eclogite		
603-2-2	Grt1-C Omph-1	746	643	708
	Grt1-C Omph-3	890	806	871
	Grt2-C Omph-2	655	550	609
B1-10	Grt1-c Omph-1	924	810	910
	Grt1-c Omph-3	804	677	772
	Grt2-c Omph2-c	819	694	778
	Grt2-c Omph2-r	855	734	819
L-4	Grt-1 Omph-1	1060	990	1026
	Grt-2 Omph-2	1039	966	1016
		Granet clinopyroxenite		
603-2-1	Grt Aug	760	698	720
JG1-36	Grt Aug	667	576	617
JG2-38	Grt Aug	664	582	612
JG3-52	Grt Aug	728	637	645
JG3-31	Grt Aug	751	674	659
JG3-65	Grt Aug	755	675	675

See Table DR 4 for abbreviations of minerals.

Table DR 6 Garnet-whole-rock Sm-Nd data and isochron age of the eclogite xenolith 603-2-2

	Sm (ppm)	Nd (ppm)	$^{147}Sm/^{144}Nd$	$^{143}Nd/^{144}Nd$		1σ	Isochron age (Ma)		1σ
Garnet	2.54	2.374	0.6471	0.512998	±	12	219	±	5
Whole rock	3.161	10.59	0.1805	0.512328	±	9			

Table DR 7 SHRIMP zircon U-Pb data on eclogite and garnet clinoproxenite xenoliths from the Xu-Huai area

Rock	Spot	U ppm	Th ppm	Th /U ratio	$^{206}Pb^*$ ppm	f206 %	Atomic ratio						Ages (Ma)			
							$^{207}Pb^*/^{235}U$	1σ	$^{206}Pb^*/^{238}U$	1σ	$^{207}Pb^*/^{206}Pb^*$	1σ	$^{206}Pb/^{238}U$	1σ	$^{207}Pb/^{206}Pb$	1σ
Eclogite	603-2.1	145	82	0.59	2.5	2.14	0.11	0.0307	0.0195	0.0012	0.0407	0.0111	124.6	7.3		
603-2-2	603-2.2	1176	1250	1.1	382	0.04	8.17	0.1194	0.3779	0.0208	0.1569	0.0005	2066	96	2423	5
	603-2.3	23	1	0.06	0.7	8.69			0.0325	0.0024			206	15		
	603-2.4	383	32	0.09	155.4	0.03	10.82	0.5951	0.4725	0.026	0.1661	0.0007	2494	113	2519	8
Garnet	603-1.1c	111	23	0.21	42.9	0.07	10.55	0.2638	0.448	0.0108	0.1709	0.0012	2386	47	2566	12
clinopyroenite	603-1.2r	891	214	0.25	15.4	0.41	0.1339	0.005	0.02	0.0005	0.0486	0.0014	127.5	2.9		
603-2-1	603-2.1	89	57	0.66	22.4	0.19	4.28	0.1156	0.2919	0.007	0.1062	0.0013	1651	34	1736	23
	603-3.1	738	247	0.35	227	0	6.09	0.1401	0.3581	0.0082	0.1233	0.0004	1973	39	2005	6
	603-4.1	626	653	1.08	230	0.02	8.75	0.2013	0.4273	0.0094	0.1485	0.0005	2294	43	2328	6
	603-5.1r	831	324	0.4	15.1	0.32	0.1669	0.0058	0.0211	0.0005	0.0575	0.0016	134.4	3		
	603-6.1	55	33	0.61	14.3	0.26	4.48	0.1299	0.3026	0.0076	0.1075	0.0016	1704	37	1757	27
	603-7.1r	498	176	0.37	8.55	1.73	0.125	0.0108	0.0196	0.0005	0.0462	0.0038	125.4	3		
	603-8.1c	643	41	0.07	260	0.03	10.86	0.2498	0.471	0.0104	0.1671	0.0007	2489	46	2529	7
	603-8.2r	233	91	0.41	89.4	0.23	9.54	0.2576	0.446	0.0116	0.1553	0.0015	2377	51	2405	16
	603-9.1	82	32	0.4	21	0.37	4.42	0.1282	0.2984	0.0072	0.1075	0.0018	1683	35	1758	31
	603-10.1	90	44	0.51	23.1	0.17	4.39	0.1229	0.2995	0.0075	0.1063	0.0011	1689	38	1736	19
Garnet	JG3-31-1	585	272	0.48	176	0.12	5.71	0.2455	0.349	0.0125	0.1185	0.0027	1932	61	1933	42
clinopyroenite	JG3-31-2	409	115	0.29	147	0.28	7.6	0.2964	0.417	0.0154	0.1323	0.002	2245	69	2129	26
JG3-31	JG3-31-3	311	186	0.62	96.8	0.06	6.33	0.2405	0.361	0.0133	0.1271	0.0011	1987	63	2059	16
	JG3-31-4	174	107	0.64	48	0.13	4.71	0.3485	0.318	0.0127	0.1071	0.0066	1782	62	1751	110
	JG3-31-5	213	175	0.85	81.7	0.69	8.56	0.4965	0.444	0.0249	0.1397	0.0024	2370	110	2223	29
	JG3-31-6	456	59	0.13	126	0.44	4.83	0.1691	0.32	0.0115	0.1095	0.0016	1789	57	1790	27
	JG3-31-7	370	406	1.14	27.6	--	0.989	0.0702	0.0855	0.0032	0.0839	0.0051	529	19	1290	120
	JG3-31-8	3594	393	0.11	1210	0.02	6.98	0.2513	0.392	0.0141	0.1293	0.0008	2131	65	2089	11
	JG3-31-9	2222	27	0.01	620	0.12	4.91	0.1817	0.324	0.0117	0.1098	0.0008	1811	57	1796	12
	JG3-31-10	949	50	0.05	219	0.43	5.97	0.2149	0.268	0.0096	0.1615	0.0007	1531	49	2471	8
	JG3-31-11	126	165	1.35	50.5	0.53	10.48	0.4297	0.461	0.0175	0.1648	0.0025	2446	77	2505	25
	JG3-31-12	101	34	0.34	30	2.08	5.14	0.3855	0.338	0.0135	0.1101	0.007	1878	64	1802	120

Table DR 7 (continued)

Rock	Spot	U ppm	Th ppm	Th /U ratio	$^{206}Pb^*$ ppm	f206 %	Atomic ratio						Ages (Ma)			
							$^{207}Pb^*/^{235}U$	1σ	$^{206}Pb^*/^{238}U$	1σ	$^{207}Pb^*/^{206}Pb^*$	1σ	$^{206}Pb/^{238}U$	1σ	$^{207}Pb/^{206}Pb$	1σ
Garnet	JG3-65-1	175	105	0.62	10.2	3.24	0.36	0.1152	0.0644	0.0026	0.041	0.0127	403	16		
clinopyroenite	JG3-65-2	1027	199	0.2	312	--	7.86	0.2908	0.353	0.0131	0.1614	0.0007	1950	62	2470	8
JG3-65	JG3-65-3	498	40	0.08	110	0.24	3.91	0.1525	0.2566	0.0092	0.1105	0.0014	1473	48	1808	24
	JG3-65-4	749	528	0.73	14.4	2.77	0.1	0.027	0.0214	0.0009	0.0343	0.0093	136.6	5.5		
	JG3-65-5	1431	152	0.11	331	0.2	4.03	0.1531	0.269	0.0097	0.1086	0.0013	1535	49	1777	21
	JG3-65-6	445	66	0.15	112	0.43	4.24	0.1611	0.292	0.0108	0.1053	0.0012	1651	53	1720	20
	JG3-65-7	303	83	0.28	7.58	12.41	0.22	0.0704	0.0259	0.0012	0.063	0.0195	164.6	7.3		
	JG3-65-8	775	92	0.12	227	0.15	5.47	0.2188	0.341	0.0122	0.1164	0.0019	1890	59	1901	29
	JG3-65-9	781	499	0.66	241	--	5.33	0.2079	0.358	0.0129	0.108	0.0015	1973	61	1765	25
Garnet	JG2-38-1	524	156	0.31	115	0.14	3.48	0.1427	0.2546	0.0092	0.0991	0.0019	1462	47	1607	36
clinopyroenite	JG2-38-2	406	483	1.23	6.68	6.67	0.1	0.044	0.0178	0.0008	0.042	0.0018	114	4.8		
JG2-38	JG2-38-3	477	180	0.39	101	0.34	3.41	0.1296	0.2458	0.0088	0.1005	0.0012	1417	46	1634	23
	JG2-38-4	586	183	0.32	132	0.35	3.64	0.142	0.2623	0.0094	0.1006	0.0013	1502	49	1635	24
Garnet	JG3-52-1	119	36	0.32	7.42	0.41	0.5	0.31	0.072	0.0042	0.05	0.03	448	25		
clinopyroenite	JG3-52-2	89	22	0.25	23	--	4.37	0.2141	0.311	0.0131	0.102	0.0026	1743	64	1660	48
JG3-52	JG3-52-3	11	2	0.2	3.46	2.26	4.6	1.38	0.341	0.0201	0.097	0.0291	1892	97	1564	560
	JG3-52-4	72	17	0.25	20.8	0.14	4.4	0.2288	0.346	0.0135	0.0922	0.0031	1916	64	1472	65
	JG3-52-5	11	0	0.03	3.61	1.49	5.8	2.204	0.354	0.0255	0.12	0.0456	1955	120	1950	670
	JG3-52-6	61	18	0.31	15.6	0	4.84	0.3098	0.305	0.0119	0.1151	0.0059	1715	59	1881	92
Garnet	JG1-36-1	10	2	0.18	0.677	47.69			0.0419	0.0024			265	49		
clinopyroenite	JG1-36-2	10	2	0.18	0.748	60.06			0.0357	0.0022			226	62		
JG1-36	JG1-36-3	10	2	0.24	0.403	29.72			0.0344	0.0022			218	26		
	JG1-36-4	9	5	0.6	0.446	45.63			0.0314	0.002			200	41		
	JG1-36-5	6	1	0.16	0.352	57.26			0.0286	0.002			182	52		
	JG1-36-6	5	2	0.3	0.778	72.23			0.047	0.0049			296	170		
	JG1-36-7	9	2	0.2	0.821	68.67			0.0341	0.002			216	87		

* Radiogenic Pb.

f206% is (common ^{206}Pb/total ^{206}Pb) x 100.

Table DR 8 SHRIMP zircon U-Pb data for felsic gneiss xenoliths from the Xu-Huai area

Rock	Spot	U ppm	Th ppm	Th /U ratio	$^{206}Pb^*$ ppm	f206 %	Atomic ratio						Ages (Ma)			
							$^{207}Pb^*/^{235}U$	1 σ	$^{206}Pb^*/^{238}U$	1 σ	$^{207}Pb^*/^{206}Pb^*$	1 σ	$^{206}Pb/^{238}U$	1 σ	$^{207}Pb/^{206}Pb$	1 σ
Leucogneiss xenolith DJG	DJG2.1	47	44	0.96	21.4	0.22	12.52	0.2754	0.524	0.0100	0.1733	0.0017	2,716	± 43	2,590	± 17
	DJG3.1	18	36	2.06	7.32	0.42	10.09	0.3330	0.465	0.0112	0.1576	0.0035	2,460	± 50	2,430	± 37
	DJG2.2	7	3	0.41	2.95	2.14	9.87	0.5527	0.49	0.0176	0.1461	0.0064	2,571	± 76	2,301	± 75
	DJG4.1	73	342	4.8	27.5	0.26	9.27	0.1947	0.4339	0.0082	0.155	0.0013	2,323	± 37	2,402	± 15
	DJG5.1	4	7	1.65	1.74	1.16	10.39	0.4883	0.457	0.0155	0.1648	0.0053	2,427	± 69	2,506	± 54
	DJG6.1	14	26	1.86	6.16	0.74	11.94	0.3582	0.499	0.0120	0.1737	0.0033	2,608	± 51	2,594	± 31
	DJG7.1	2	4	1.74	1.2	2.46	12.4	1.3640	0.579	0.0261	0.155	0.0147	2,946	±110	2,399	± 160
	DJG8.1	119	47	0.41	46	0.5	10.3	0.1957	0.4486	0.0081	0.1665	0.0012	2,389	± 36	2,523	± 12
	DJG2.1	10	17	1.77	4.1	0.88	11.66	0.5247	0.467	0.0131	0.1812	0.0063	2,468	± 58	2,664	± 57
	DJG9.1	15	27	1.93	6.08	0.48	10.9	0.3161	0.478	0.0115	0.1654	0.0028	2,519	± 49	2,512	± 28
	DJG10.1	19	102	5.66	7.96	0.42	11.57	0.3124	0.496	0.0109	0.1691	0.0027	2,598	± 48	2,548	± 27
	DJG11.1	11	20	1.86	4.53	1.11	9.72	0.4860	0.473	0.0180	0.149	0.0049	2,497	± 78	2,334	± 56
	DJG12.1	25	132	5.48	10.3	0.52	10.54	0.3057	0.48	0.0106	0.1592	0.0030	2,527	± 45	2,447	± 33
	DJG13.1	11	19	1.85	4.47	0.6	11.45	0.5153	0.474	0.0180	0.1751	0.0044	2,502	± 79	2,607	± 41
	DJG14.1	37	199	5.59	14	0.4	9.43	0.2358	0.4399	0.0088	0.1555	0.0022	2,350	± 39	2,407	± 24
	DJG15.1	30	175	5.97	12.1	0.81	10.31	0.2681	0.4623	0.0097	0.1617	0.0026	2,450	± 42	2,474	± 26
	DJG16.1	12	30	2.53	4.58	0.61	8.75	0.3413	0.435	0.0109	0.1458	0.0044	2,330	± 49	2,297	± 52
Melagneiss xenolith EJG	EJG2.1	33	63	1.98	13.4	0.12	10.49	0.2413	0.47	0.0094	0.1619	0.0018	2,483	± 41	2,476	± 18
	EJG3.1	25	30	1.27	9.18	0.23	9.31	0.2607	0.4325	0.0095	0.1561	0.0027	2,317	± 43	2,414	± 29
	EJG4.1	23	21	0.98	9.77	--	11.92	0.3218	0.505	0.0116	0.1713	0.0022	2,635	± 50	2,570	± 22
	EJG5.1	52	74	1.49	21.5	0.04	11.9	0.2618	0.4831	0.0092	0.1787	0.0020	2,541	± 40	2,641	± 19
	EJG5.2	15	8	0.54	4.89	1.5	8.1	0.3726	0.3742	0.0094	0.1569	0.0060	2,049	± 44	2,423	± 64
	EJG6.1	21	11	0.56	8.63	0.61	10.78	0.3989	0.482	0.0164	0.1621	0.0026	2,538	± 70	2,478	± 26
	EJG7.1	7	2	0.27	2.92	1.44	10.42	0.4689	0.461	0.0138	0.1641	0.0054	2,443	± 61	2,498	± 56
	EJG8.1	16	16	1.02	6.63	0.12	11.19	0.3581	0.489	0.0112	0.166	0.0035	2,567	± 49	2,518	± 36
	EJG9.1	23	25	1.12	8.98	0.35	9.89	0.2571	0.4604	0.0097	0.1558	0.0023	2,441	± 43	2,410	± 25
	EJG10.1	16	23	1.46	6.64	0.28	10.95	0.3504	0.47	0.0127	0.1692	0.0027	2,482	± 56	2,550	± 28
	EJG11.1	33	15	0.46	13.3	0.17	10.72	0.2466	0.4692	0.0094	0.1658	0.0018	2,480	± 41	2,515	± 19
	EJG12.1	72	62	0.89	28.2	0.13	10.62	0.2124	0.4582	0.0082	0.1681	0.0011	2,432	± 37	2,539	± 11
	EJG13.1	33	15	0.46	14.9	0.23	11.96	0.5860	0.526	0.0200	0.1648	0.0049	2,726	± 85	2,506	± 51
	EJG14.1	23	20	0.9	7.63	0.67	8.41	0.2355	0.3854	0.0085	0.1583	0.0030	2,101	± 39	2,438	± 31
	EJG15.1	42	43	1.07	16.9	0.13	10.5	0.2520	0.471	0.0094	0.1617	0.0019	2,488	± 41	2,473	± 21

* Radiogenic Pb.

f206% is (common ^{206}Pb/total ^{206}Pb) x 100.

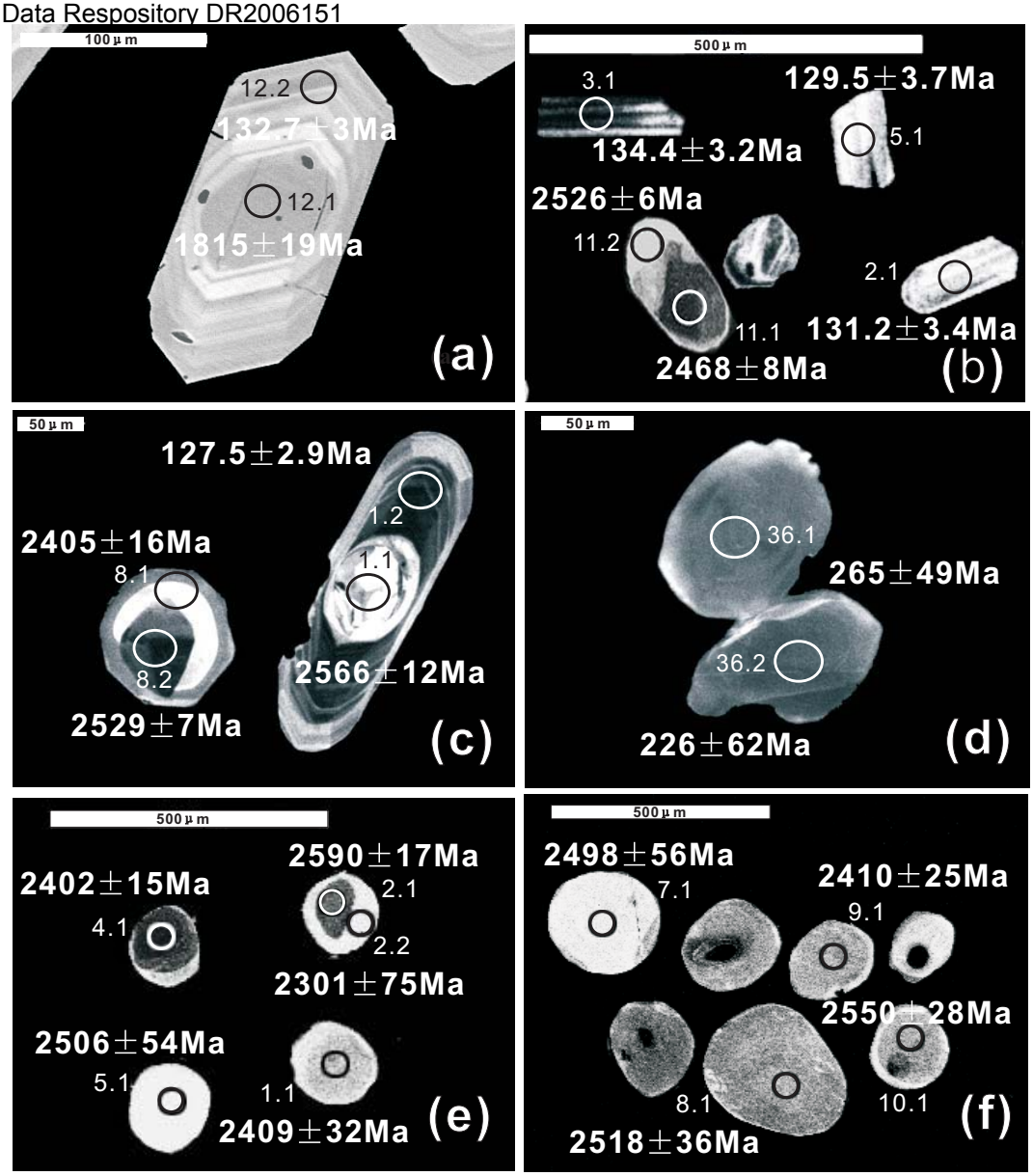
100 µm
12.2
132.7±3Ma
12.1
1815±19Ma
(a)
500 µm
3.1
129.5±3.7Ma
134.4±3.2Ma
5.1
2526±6Ma
11.2
2.1
11.1
131.2±3.4Ma
2468±8Ma
(b)
50 µm
127.5±2.9Ma
1.2
2405±16Ma
1.1
8.1
8.2
2566±12Ma
2529±7Ma
(c)
50 µm
36.1
265±49Ma
36.2
226±62Ma
(d)
500 µm
2590±17Ma
2402±15Ma
2.1
4.1
2.2
2301±75Ma
2506±54Ma
5.1
1.1
2409±32Ma
(e)
500 µm
2498±56Ma
7.1
2410±25Ma
9.1
2550±28Ma
8.1
10.1
2518±36Ma
(f)

Figure DR 1

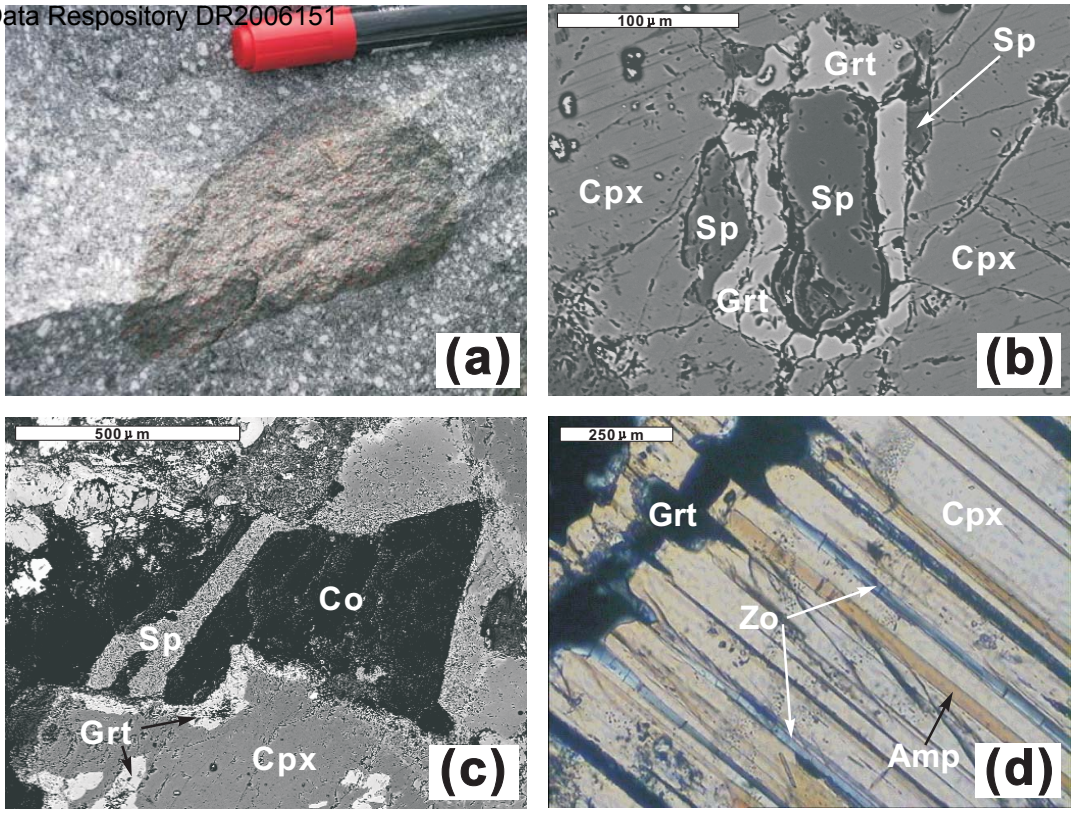
(a)
100 µm
Grt
Sp
Cpx
Sp
Sp
Cpx
Grt
(b)
500 µm
Co
Sp
Grt
Cpx
(c)
250 µm
Grt
Cpx
Zo
Amp
(d)

Figure DR 2

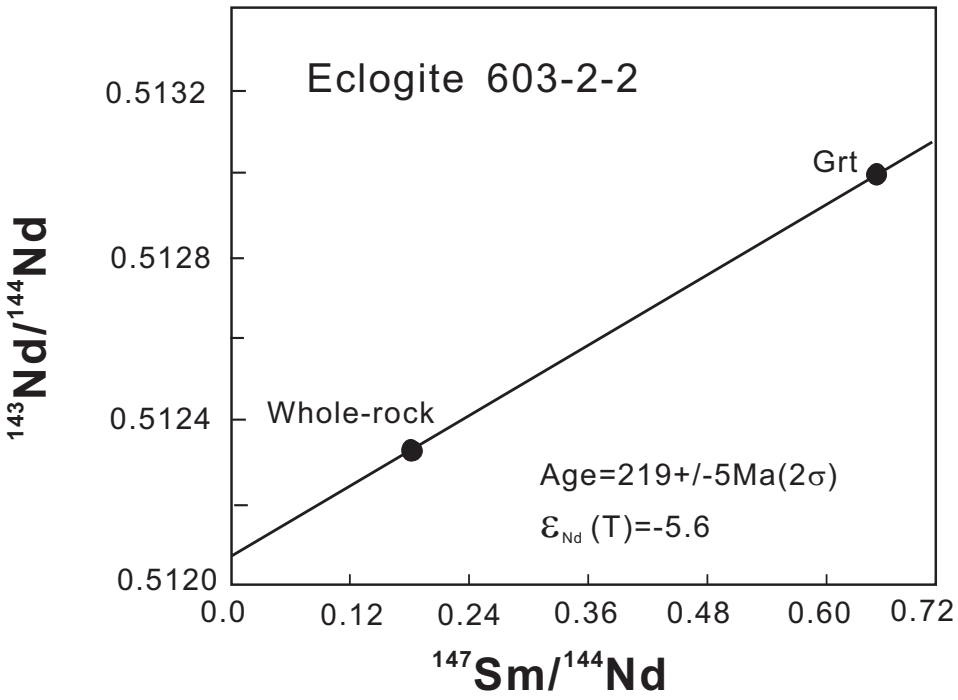
Eclogite 603-2-2
Grt
Whole-rock
Age=219+/-5Ma(2σ)
εNd (T)=-5.6
0.5132
0.5128
0.5124
0.5120
0.0
0.12
0.24
0.36
0.48
0.60
0.72
143Nd/144Nd
147Sm/144Nd

Figure DR 3

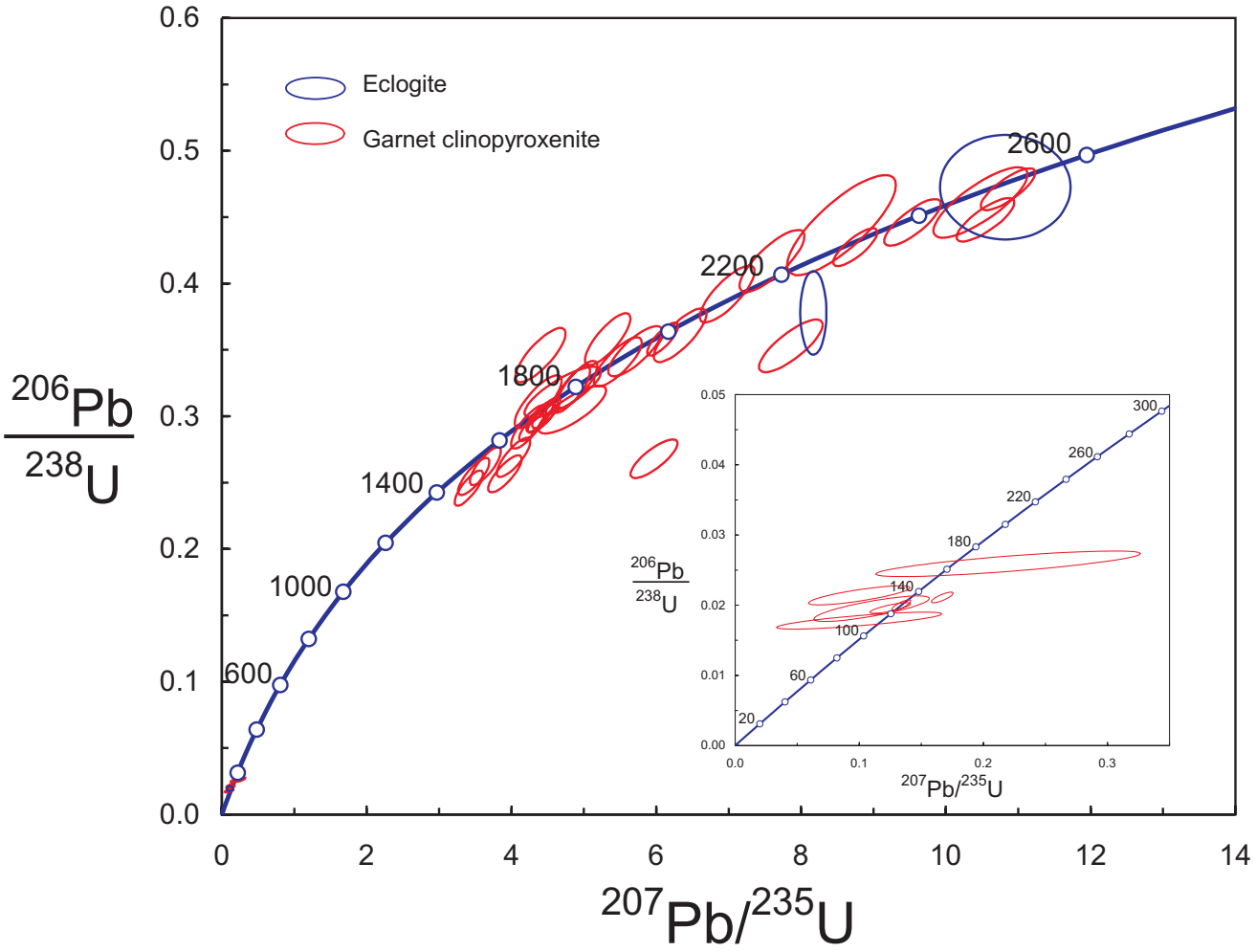
Eclogite
Garnet clinopyroxenite
600
1000
1400
1800
2200
2600
$^{206}Pb/^{238}U$
$^{207}Pb/^{235}U$
0.0
0.1
0.2
0.3
0.4
0.5
0.6
0
2
4
6
8
10
12
14
20
60
100
140
180
220
260
300
0.00
0.01
0.02
0.03
0.04
0.05
0.0
0.1
0.2
0.3

Figure DR 4

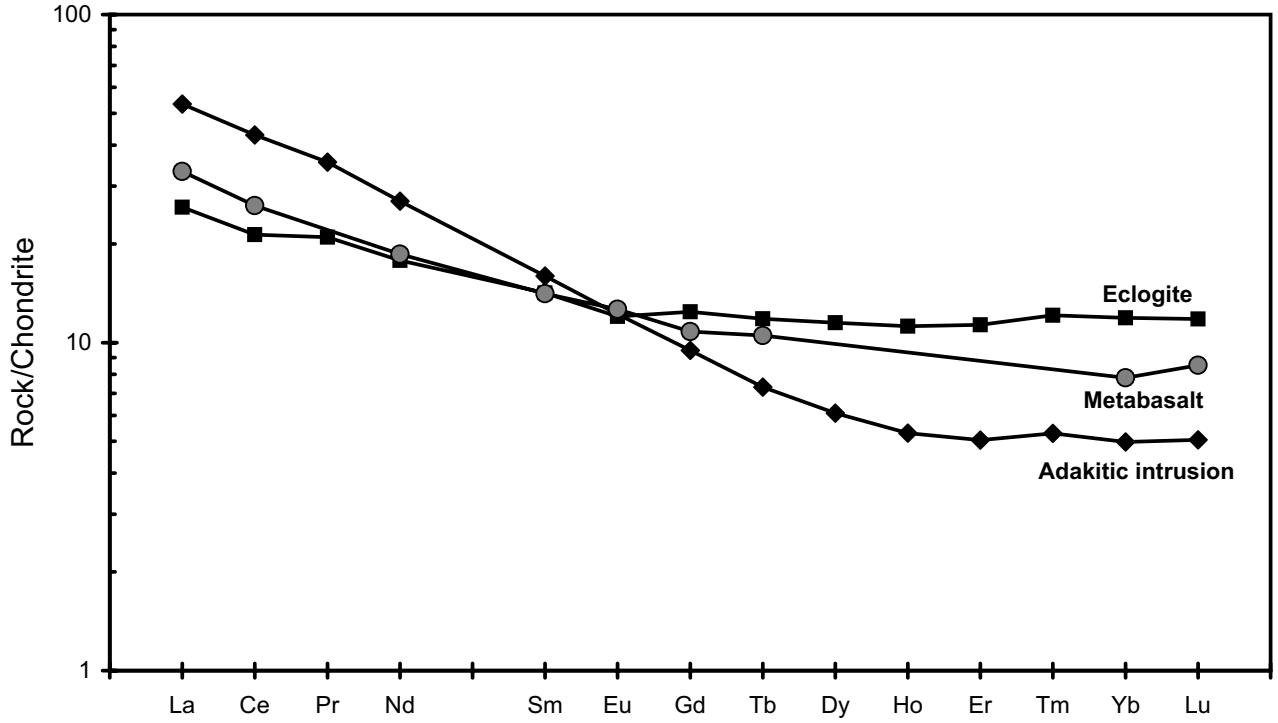
100
10
1
Rock/Chondrite
La
Ce
Pr
Nd
Sm
Eu
Gd
Tb
Dy
Ho
Er
Tm
Yb
Lu
Eclogite
Metabasalt
Adakitic intrusion

Figure DR5

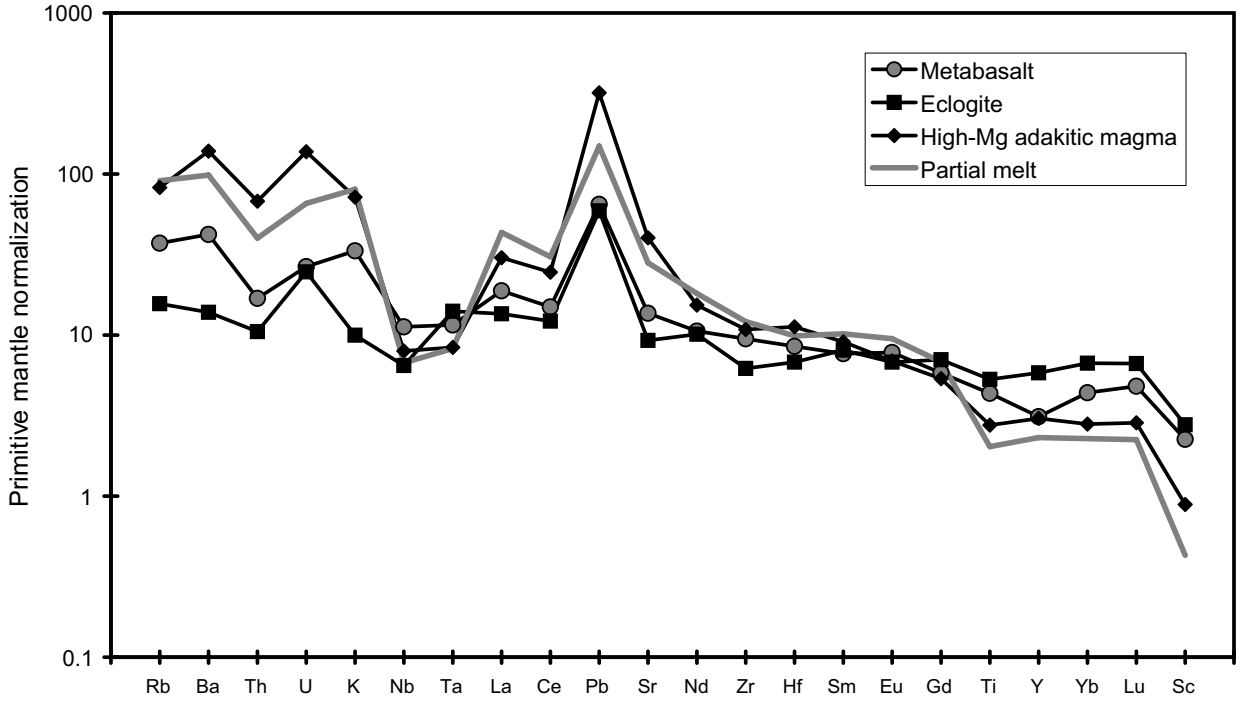
1000
100
10
1
0.1
Primitive mantle normalization
Metabasalt
Eclogite
High-Mg adakitic magma
Partial melt
Rb
Ba
Th
U
K
Nb
Ta
La
Ce
Pb
Sr
Nd
Zr
Hf
Sm
Eu
Gd
Ti
Y
Yb
Lu
Sc

Figure DR6

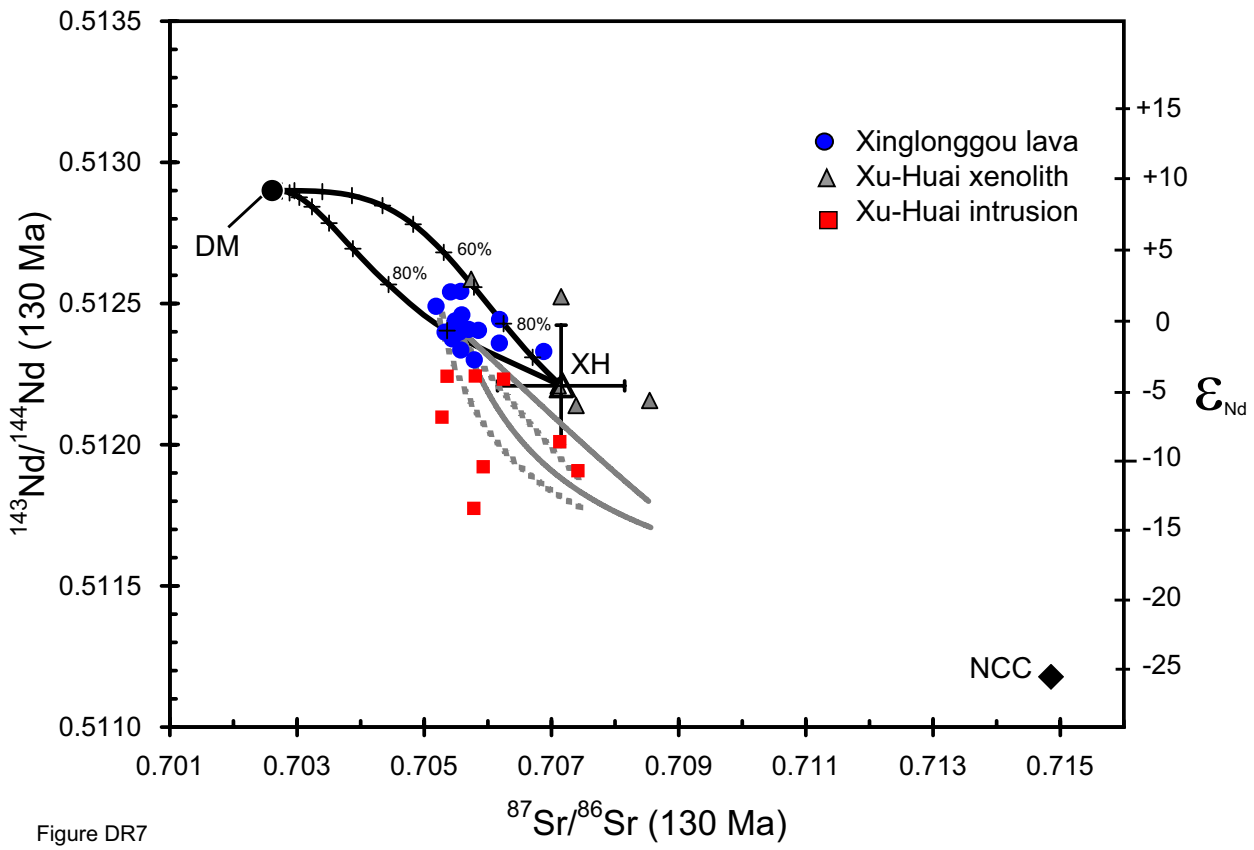
0.5135
0.5130
0.5125
0.5120
0.5115
0.5110
$^{143}Nd/^{144}Nd$ (130 Ma)
0.701
0.703
0.705
0.707
0.709
0.711
0.713
0.715
$^{87}Sr/^{86}Sr$ (130 Ma)
+15
+10
+5
0
-5
-10
-15
-20
-25
ε_{Nd}
Xinglonggou lava
Xu-Huai xenolith
Xu-Huai intrusion
DM
60%
80%
80%
XH
NCC

Figure DR7